

THE LIFESPAN OF HEAT PIPES ON IO, MODELED WITH MELT MIGRATION. J. Schools¹ and L. G. J. Montési¹, ¹Department of Geology, University of Maryland, College Park (jschools@umd.edu; montesi@umd.edu)

Introduction: Jupiter's moon Io possesses the largest surface heat flux of any terrestrial body in the solar system, at $\sim 2.24 \text{ W m}^{-2}$ on average, or more than 20 times the average Earth heat flux [1]. Io likely transports heat through advection as magma rises from deeply rooted vents to the surface [2]. As the magma flows on to the surface, it spreads and cools. Subsequent flows bury older flows and the lithosphere subsides due to the weight. Buried flows at the base of the lithosphere heat through conduction, melt, and start the cycle again [2].

Io's extreme volcanism buries the surface at least 200 meters, and up to 140 km, per million years [3,4]. Surface features of Io are therefore very short lived, geologically speaking, but what about interior structures? Here we investigate the longevity of heat-pipes using simple models involving melt migration.

Model: Using the finite element code ASPECT 2.0.1 [5,6], we model the evolution of an idealized, preexisting heat-pipe in an Ionian lithosphere in two dimensions. For incompressible models with melt migration, ASPECT operates by solving the following equations for conservation of mass and momentum (Eq 1-3), fluid content (Eq. 4), and temperature/heating (Eq. 5), describing the behavior of silicate melt moving through and interacting with a viscously deforming host rock:

$$-\nabla \cdot (2\eta \dot{\epsilon}) + \nabla p_f + \nabla (\sqrt{K'_D} \bar{p}_c) = \bar{\rho} \mathbf{g} \quad (1)$$

$$\nabla \cdot \mathbf{u}_s - \nabla \cdot K_D \nabla p_f = -\nabla \cdot (K_D \rho_f \mathbf{g}) + \Gamma \left(\frac{1}{\rho_f} - \frac{1}{\rho_s} \right) \quad (2)$$

$$\sqrt{K'_D} \nabla \cdot \mathbf{u}_s + \frac{K'_D \bar{p}_c}{\xi} = 0 \quad (3)$$

$$\frac{\partial \phi}{\partial t} + \mathbf{u}_s \cdot \nabla \phi = \frac{\Gamma}{\rho_s} + (1 - \phi)(\nabla \cdot \mathbf{u}_s) \quad (4)$$

$$\bar{\rho} C_p \left(\frac{\partial T}{\partial t} + \mathbf{u}_s \cdot \nabla T \right) - \nabla \cdot k \nabla T = \rho_s H + T \Delta \Sigma \quad (5)$$

See [5,6,7,8] for more details and derivations. The melting model follows the parameterization of [9] for dry peridotite.

In Eq (5), this model takes into account release and consumption of latent heat due to melting and freezing and constant heating. Heat generation in this model is not radiogenic heating, but rather an approximation of the tidal heating in the asthenosphere of Io. For simplicity, it is assumed to be constant throughout the asthenosphere.

The model setup consists of a 100 km by 100 km box representing a ~ 50 km thermal lithosphere, and the upper 50 km of a molten asthenosphere. The initial temperature profile of the lithosphere is set to the steady-

state solution of the heat equation in a continuously buried lithosphere:

$$T = T_s + \Delta T \frac{e^{z/l} - 1}{e^{d/l}} \quad (6)$$

where ΔT is the temperature difference between the base of the lithosphere and the surface, T_s is the surface temperature, d is the lithosphere thickness, and $l = \alpha/v$, where α is the thermal diffusivity, and v is the burial rate [2]. The temperature of the asthenosphere, at depths greater than d , is initially set to 1500 K. The top temperature is 113 K and the bottom remains at 1500 K.

The heat-pipe itself is defined as a section of the lithosphere on the left hand side of the model with the same temperature as the asthenosphere. The model set up is approximating an axisymmetric geometry, therefore the width of the heat-pipe section in the model represents the radius of the heat-pipe. A small slope is added to the base of the lithosphere (the thickness of the lithosphere increases slightly away from the pipe) to facilitate melt flow toward the heat pipe.

The side boundaries are free slip and insulating. The bottom boundary is open to solid and melt flow. The top boundary has an imposed solid flow of 1 cm/yr downward as a simple approximation of burial.

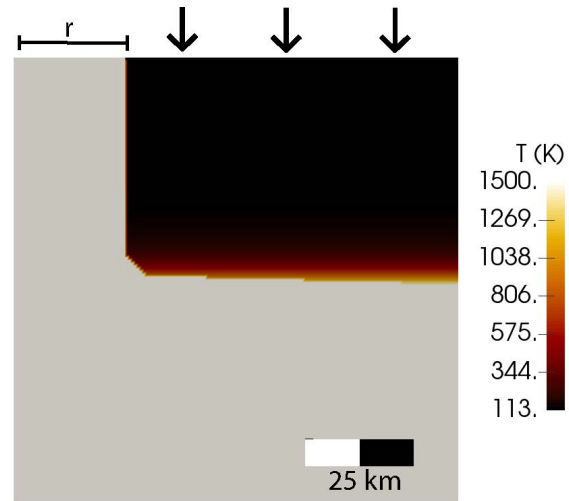


Figure 1 - Model set up. Three models with differing heat-pipe radii (r) were run. Solid material flows in from the top of the box at 1 cm/yr, representing burial.

Results: Preliminary results are presented for heat-pipes with radii of 5, 10, and 25 km. In all three of the models, the same two primary processes occur.

First, the solid lithosphere flows downward and melts at the lithosphere/asthenosphere boundary. This

melt flows upslope to the heat-pipe, however in this model setup, the slope of the lithosphere is small to permit rapid lateral transport along the base of the lithosphere, and the newly generated melt accumulates in a decompaction channel [10,11]. In addition, the melt present in the asthenosphere rises buoyantly, also feeding the decompaction channel.

Second, the heat pipe loses heat to the surrounding cold lithosphere at a faster rate than heat is supplied by rising melt. Therefore, the heat pipe cools and the melt it contains crystallizes, shrinking the radius of the heat pipe. The models described here have not run long enough to observe the eventual closure of the heat pipe. However, a preliminary calculation with a 1 km diameter pipe documents closure after 1800 years. The pipe pinches off near its base, leaving a magma body in the shallowest levels of the lithosphere.

The Stefan Problem: In order to determine the amount of time until heat pipe closure, we compare our numerical model with a Stefan problem, as applied to a cooling and crystallizing dike [12,13]. Heat is transferred by diffusion between a molten body and a solid medium in contact with it, with an additional heat source related to crystallization. The position of the solidifying wall y_m , changes over time t as:

$$y_m = 2\lambda_1\sqrt{\kappa t} \quad (7)$$

where κ is the thermal diffusivity and λ_1 is a constant value corresponding to the solidification boundary, given by

$$\frac{L\sqrt{\pi}}{c(T_m - T_0)} = \frac{e^{\lambda_1^2}}{\lambda_1 \text{erf} \lambda_1} \quad (8)$$

where L is the latent heat of fusion, T_m is the temperature of the molten material, and T_0 is the temperature of the solid material.

The positions of the 25 km radius heat-pipe in the numerical model corresponds well to the calculated values, however the 5 and 10 km shrink at a faster rate in the model than in the calculation. This is likely due to the finite size of the heat pipe and heat loss from the opposite wall. The times for full heat-pipe closure are expected to be 250,000 years for a 5 km radius, 900,000 years for a 10 km radius and 6.1 million years for the 25 km radius.

Discussion: Despite the large size used in these models, heat-pipes appear to have a relatively short lifespan, shorter than the time needed to renew the lithosphere by burial (2.5 million years in these calculations). If patera size is at all related to heat pipe radius, a large eruptive center such as the 200 km diameter Loki Patera could last 90 million years, however smaller heat pipes are expected to close relatively quickly. Processes that may help keeping heat pipes open include shear heating, which was not included in this model. Shear

heating would be particularly important at the heat pipe wall, where strain rate was elevated.

Preliminary models show that a fully closed heat pipe leaves behind a remnant, cone-shaped structure at the base of the lithosphere. Asthenospheric melt would likely collect and focus here. Heat release due to crystallization of melt may alter the thermal profile allowing melt to rise through the lithosphere [14,15], facilitating the reactivation of an older heat-pipe. If heat pipes are so thin that they close over a time scale of a few decades, volcanic activity may still continue episodically at the same location due to this potential for reactivation. For example, Loki has been observed have activity cycles with 1.5 year period [16], implying a 13 m thick heat pipe.

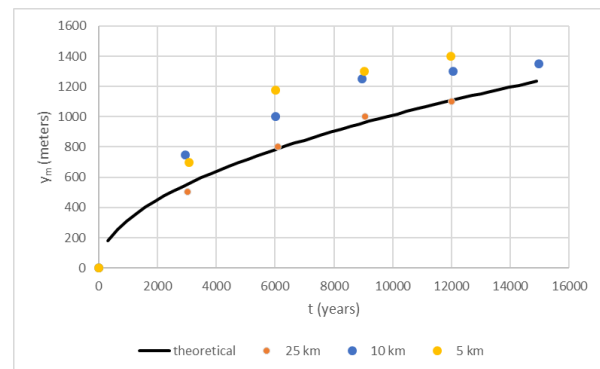


Figure 2 - Position of heat-pipe wall at time t , in the numerical model (colored dots) and as a solution to the Stefan problem (black line).

References: [1] Lainey V. et al. (2009) *Nature*, 459, 957–959. [2] O'Reilly T. C. and Davies G. F. (1981) *GRL*, 8, 313-316. [3] Phillips C. B. (2000) PhD Thesis. University of Arizona [4] Johnson T.V et al. (1979) *Nature*, 280, 746-750. [5] Heister T. et al. (2017) *GJI*, 191, 12-29. [6] Bangerth W. et al. (2018) *ASPECT User Manual*. [7] Dannberg J. and Heister T. *GJI*, 207, 1343-1366. [8] Dannberg J. et al. (2018) arXiv:1810.10105v1. [9] Katz R.F. et al. (2003) *G-cubed*, 4, 1073. [10] McKenzie D. (1984) *J. Petrol.*, 25, 713-765. [11] Sparks D. W. and Parmentier E. M. (1991) *EPSL*, 105, 368-367. [12] Stefan J. (1891) *Ann. Physik Chem.*, 42, 269-286. [13] Spohn T. (1988) *JGR*, 93, 4880-4894. [14] Schools J. and Montési L. G. J. (2017) *LPSC 48*, Abstract #2723. [15] Schools J. and Montési L. G. J. (2018) *LPSC 49*, Abstract #2301. [16] Rathbun, J. A. et al. (2002) *GRL*, 29, 1443.

Acknowledgements: This research was supported by a NASA Earth and Space Science Fellowship 80NSSC17K0486. ASPECT is hosted by the Computational Infrastructure for Geodynamics (CIG) which is supported by the National Science Foundation award EAR-1550901.